Continuous Kneading of Electrically Conductive Composite Materials and Evaluation of Filler Dispersion State

Continuous Kneading for Electrically Conductive Composite Materials and Evaluation of Filler Dispersion State

Keijiro Terashita, Tetsuya Tanaka, Kiyohiko Nishimura,
and Kei Miyanami

Using stainless steel fiber and metalized glass fiber as electrically conductive fillers, electrically conductive composite resins were prepared by continuous kneading. Among the factors affecting the electroconductivity of electrically conductive composite material are the filler dispersion state and filler length in the matrix resin. The key to excellent electroconductivity is to form an electrically conductive network ensuring long filler length, a uniform filler distribution and filler orientation in every direction. As quantitative indexes of the filler dispersion state, the fractal dimension and direction ratio were used.

A good filler dispersion state was obtained when the fractal dimension was high and the direction ratio was low. Electrically conductive composite resin was found to show excellent electroconductivity, irrespective of filler type, when the filler length was long, the fractal dimension was high and the direction ratio was low. A good filler distribution and orientation with long filler length were obtained when the number of paddle revolutions Nt is low, the ratio τ / μ of shearing stress τ to resin viscosity μ is high and the ratio μ /Vh of μ to holdup Vh was low.

1. Introduction

In recent years there have been active R & D activities for composite materials offering a new function by a combination of a matrix resin and a filler. With the aim of overcoming the problem of electromagnetic interference (EMI), we have already studied various electrically conductive composite resins[1-6]. In these studies, fibrous electrically conductive fillers were dispersed in matrix resin by continuous kneading under various sets of operating conditions to identify optimum conditions for excellently electrically conductive composite resins.

Factors affecting the electroconductivity of electrically conductive composite resin include the dispersion state of filler and filler length in the matrix resin. Previous studies examined the relationship between electroconductivity and filler length[2, 3]. Also, the dispersion state of filler has often been evaluated visually by light microscopy etc. or indirectly on the basis of electroconductivity deviation or in continuous kneading, subject material fluidity. However, for efficient design of a composite material, it is mandatory to quantitatively evaluate the dispersion state of filler.

There have recently been attempts to apply the theory of fractal to the quantitative evaluation of particle or aggregate morphology[7-9]. Fractal, an idea based on selfsimi-

Keijiro TERASHITA, Tetsuya TANAKA, Kiyohiko NISHIMURA
and Kei MIYANAMI

larity, offers a unique representation, by simple analysis, of complex morphology as cannot be dealt with by conventional geometry.

This paper reports on the effects of filler type on electroconductivity or network formation state as expressed by quantitative representation of filler length or filler dispersion state in electically conductive composite resins prepared by continuous kneading of two kinds of fibrous electrically conductive fillers. As a quantitative index of filler dispersion state in the matrix resin, the fractal dimension was used. Also discussed is the relationship between factors involved in network formation and kneaded product fluidity as determined by measuring kneading torque, resin's apparent viscosity and residence time during continuous kneading.

2. Experimental design

2.1. Experimental apparatus

The continuous kneading machine used in this study, outlined in the previous paper[6], is briefly described below (see Figure 1). A tight kneading vessel (length 0.165 m, capacity 8.844×10^{-5} m[3]) houses two kneading shafts revolving at the same speed in the same direction. Helical or convex paddles, incorporated in the kneading shafts, perform kneading. A total of 28 paddles are arranged on each shaft, of which 20 were helical paddles, which are recognized as offering short residence time and causing less cutting of fibrous filler during kneading.
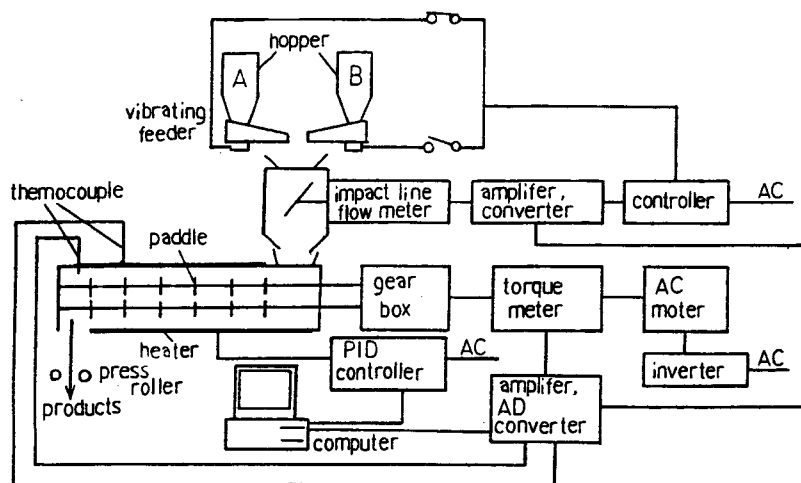

Fig. 1 Schematic diagram of continuous kneading system.

To design a uniform electrically conductive composite material, the starting materials should be fed at constant feed rate under stationary temperature conditions during the continuous kneading operation[6]. For this reason, starting material feed and kneading vessel heating were controlled by PID as follows: First, the starting materi-

als were fed to the kneading vessel inlet from the hopper via an electromagnetic feeder. Between the feeder and kneading vessel was arranged an impact line flowmeter. The flow rate signal detected by the flowmeter was fed back to the controller, which sent a control signal to the electromagnetic feeder to control the feed rate.

Kneading vessel inside temperature was measured and controlled as follows: A band heater was fixed around the kneading vessel. Heater temperature and kneading vessel inside temperature (hereinafter also referred to as kneading temperature) were measured by thermocouples set between the heater and kneading vessel and near the kneading vessel outlet, respectively. Kneading vessel inside temperature was kept constant (preset temperature ± 2 K) by PID control of heater temperature. Data on the controlled feed rate, heater temperature and kneading temperature were output to a personal computer and recorded automatically. Agitating (kneading) torque was also measured by a torque meter, the data obtained being output to the personal computer and recorded automatically.

2.2 Samples

Table 1 shows the physical property data on the matrix resins and fillers used in the experiments. The previous paper[5] reported that polystyrene (PS) resin ranked highest in electrically conductive composite resin electroconductivity among ABS resin, PS resin and polypropylene (PP) resin as matrix resins. PS resin was thus selected for the present study. Two types of electrically conductive fillers were used: a glass fiber filler, coated with Ni-Cu-Ni (length 3 mm, diameter 13 μm, a bundle of 2300 filaments) and a stainless steel fiber filler (length 5 mm, diameter 8 μm, a bundle of 5000 filaments). The glass fiber (GF) filler remain linear even after kneading, though it is prone to folding upon shearing action, while the stainless steel fiber (SF) filler tends to be bent, though it is highly resistant to cutting.

Table 1 Properties of the matrix resin and the fillers used in kneading.

	PS resin	Glass fiber	Stainless steel fiber
Softening point [K]	513	—	—
Specific gravity [—]	1.04	3.6	7.9
Specific resistivity [$\Omega \cdot$m]	—	10^{-7}	7.2×10^{-4}
Tensile strength [kg/mm²]	—	15	106~140
Shape	Pellets ($\phi 2.3 \times$ 3 mm)	Bundles of 2300 chops ($\phi 13 \mu$m × 3 mm) coated with Ni-Cu-Ni layers	Bundles of 5000 chops ($\phi 8 \mu$m × 5mm)

2. 3 Methods

a) Kneading experiment and determination of volume specific resistivity

After the kneading vessel was heated by the heater until the kneading vessel inside temperature became constant at the preset level, the matrix resin alone was fed at constant rate from the hopper to the kneading vessel. Upon reach of a given level of agitation torque, a resin-filler premixture was step by step fed at constant rate. The kneaded mixture discharged from the kneading vessel outlet was sampled periodically and shaped into a 5 mm thick piece using a press roller. Each obtained sample was molded into 18×18 mm size, and the resistance value R_v was measured in two different directions, as shown in Figure 2.
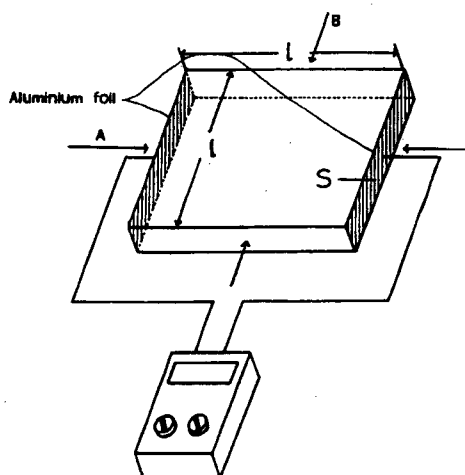

Fig. 2 Schematic diagram of measurement of resistance value

If we write cut area S and distance between electrodes l, volume specific resistivity ρ_v can be obtained as follows:

$$\rho_v = (S/l) \cdot R_v \qquad \qquad \cdots\cdots (1)$$

Volume specific resistivity was measured on 15 samples, the mean value $\overline{\rho}_v$ being used to evaluate the specific resistivity. Volume speific resistivity, an index of the electroconductivity of the kneaded mixture, decreases as electroconductivity increases.

The kneading experiment was conducted at varied starting material feed rates and kneading temperatures.

b) Filler length determination

Mean filler length was determined as follows: For the 15 samples obtained from the kneading experiment, mean volume specific resistivity $\overline{\rho}_v$ was calculated, the sample having a volume specific resistivity ρ_v closest to $\overline{\rho}_v$ was selected. Next, after the resin was dissolved in an organic solvent mixture (1:1 mixture of toluene and methyl ethyl ketone), the filler filaments was separated. Under 20-fold magnification using a pro-

jector, the filler was observed for filler length with respect to 200 filaments for the stainless steel fiber filler and 400 filaments for the glass fiber filler, and the mean was calculated.

c) Evaluation of filler distribution
  Figure 3 is a schematic diagram of the image analyzer used to determine the fractal
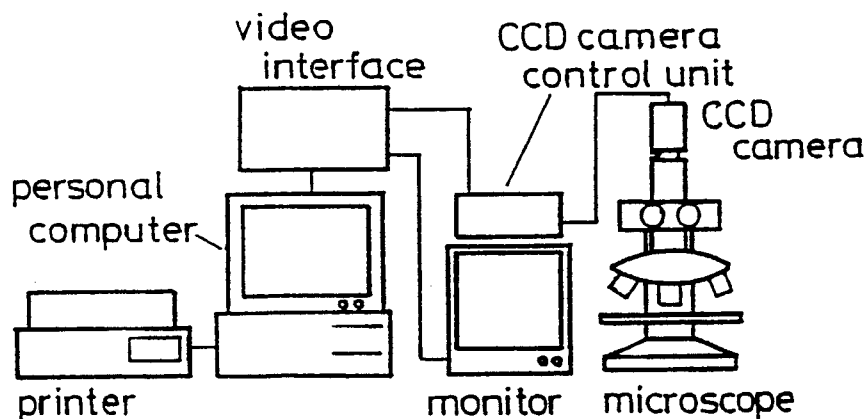

Fig. 3 Schematic diagram of image analyzer system.

dimension. A cross-section of a kneaded product prepared as directed in 2.2.(a) was observed using a light microscope, the obtained image being photographed using a CCD camera. The analogue signal from the CCD is digitized and sent to the compu-ter via a video interface. The obtained information was subjected to a smoothing treatment to remove noise and then converted to a binary data to locate the filler re-gion on the image. After these processes, the image was displayed on CRT and used to calculate the fractal dimension. In this analysis, magnifying power was optimized at 50 folds to observe the filler distribution over an as wide range as possible. Based on this dealt image, the fractal dimension was determined as a quantitative representa-tion of the filler dispersion state as follows:
  First, the dealt image was divided into $n \times n$ segments ($2 \leqq n \leqq 80$) to yield n^2 seg-ments. Next, for each segment, the area ratio Sf of filler was calculated as follows:

$$Sf = Af/A \qquad\qquad \cdots\cdots (2\text{-}1)$$

where Af is the area of the filler region in a single segment, and A is the total area of the same segment. Coefficient of variance $Ds(n)$ was calculated from the mean of percent area for an arbitrary n ($\overline{Sf}(n)$) and standard deviation $\sigma s(n)$ as follows:

$$Ds(n) = \sigma s/\overline{Sf}(n) \qquad\qquad \cdots\cdots (2\text{-}2)$$

  Figure 4 shows an example binary logarithmic plot of $Ds(n)$ versus $1/n$. If $Ds(n)$

Keijiro TERASHITA, Tetsuya TANAKA, Kiyohiko NISHIMURA
and Kei MIYANAMI

and $1/n$ bears the relationship:

$$Ds(n) \propto (1/n)^{-D} \qquad \cdots\cdots (2\text{-}3)$$

then the filler dispersion state can be expressed by fractal dimension.

Since a linearity is present over the range of $2 \leqq n \leqq 80$, as seen in Figure 4, fractal dimension D can be calculated from the gradient. The filler dispersion state improves as D increases.

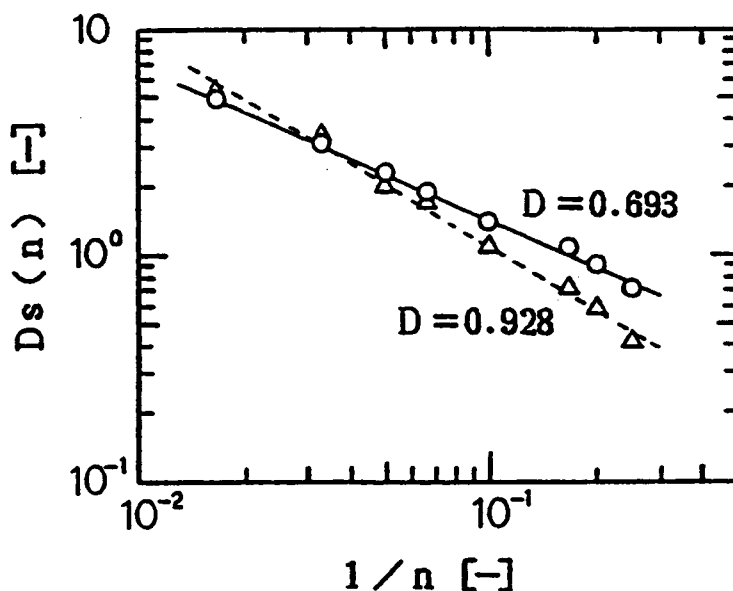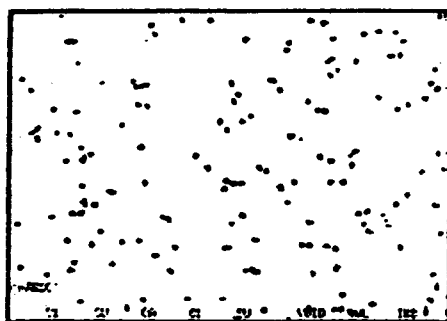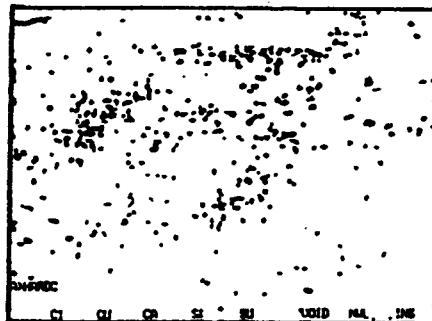Figure 5 shows a dealt image showing a filler dispersion state and its fractal dimen-

Fig. 4 Example for calculation of fractal dimension

(a)　D = 0.907　　　　　(b) D = 0.462

Fig. 5 Dealt images showing fillers dispersion state and its fractal dimension D

sion D. In Figure 5, black spots and lines indicate electrically conductive fillers, while the white portions indicate the matrix resin. A high value for fractal dimension demonstrates a visually good dispersion state with no filler aggregation. In other words, the parameter D proved useful in quantitative determination of filler dispersion state.

3. Results and Discussion

3. 1. Relationship between electroconductivity and operating conditions

Figure 6 and 7 show the relationships between kneaded product electroconductivity and starting material feed rate Fi and kneading temperature T, respectively, found in the continuous kneading experiment using glass fiber (GF) and stainless steel fiber (SF) as electrically conductive fillers. The filling ratio for electrically conductive filler was optimized for excellently electrically conductive composite resins[2, 4]. Specifically, the filling ratio was 40wt% for the glass fiber filler and 10 wt% for the stainless steel fiber filler. From Figure 6, it is seen that the mean volume specific resistivity $\bar{\rho}_v$ decreased (electroconductivity improved) as Fi increased, for both fillers, though somewhat different figures were obtained. However, when Fi was further increased (Fi=8.33×10^{-4} kg/s for the stainless steel fiber filler, Fi=7.5×10^{-4} kg/s for the glass fiber filler), the electroconductivity lowered. From Figure 7, it is seen that $\bar{\rho}_v$ decreased (electroconductivity improved) as kneading temperature T increased.
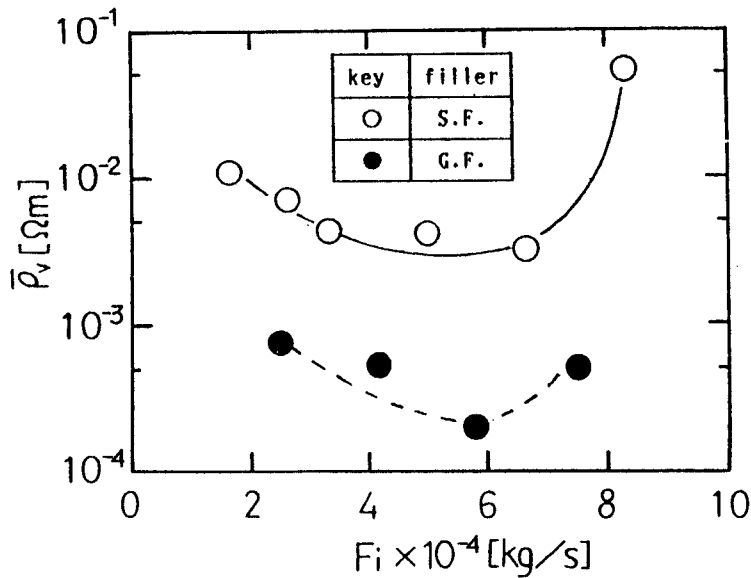

Fig. 6 The relationship between kneaded product electric conductity and starting material feed rate Fi.

Keijiro TERASHITA, Tetsuya TANAKA, Kiyohiko NISHIMURA
                                  and Kei MIYANAMI
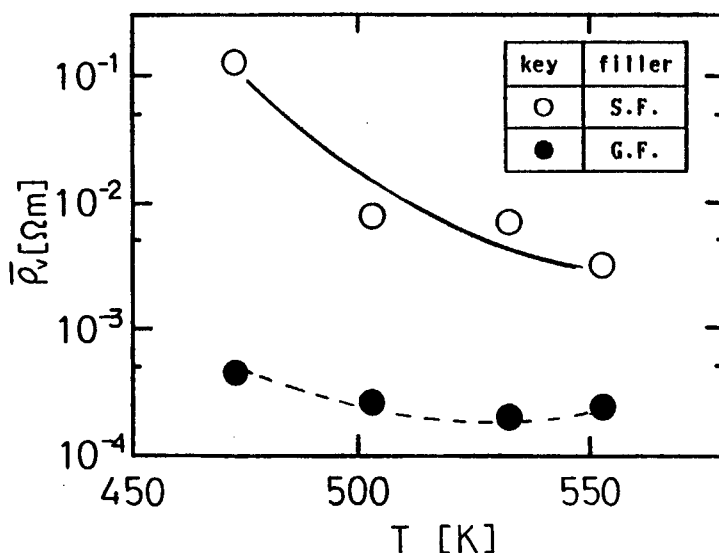

Fig. 7 The relationship between kneaded product electric conductivity and
        kneading temperature T.

Some factors (filler length, fractal dimension, direction ratio) affecting the electro-conductivity of electrically conductive composite resin were correlated to operating conditions.

3. 2. Electroconductivity-controlling factors

The electroconductivity of electrically conductive composite resin is thought to depend on the state of formation of electrically conductive network by the filler. When using a fibrous electrically conductive filler, filler length and filler dispersion state in the matrix resin are the key factors of network formation[2, 3, 6]. To design an excellently electrically conductive composite resin, it is necessary to ensure sufficient filler length, uniform filler distribution and filler orientation in every direction. Such a dispersion state is expected to increase the number of filler contact points and lead to formation of a good electrically conductive network. These factors were correlated to operating conditions as follows:

a) Effect of filler length on electroconductivity

Figure 8 shows the relationship between dimensionless mean filler length $\bar{L}_F/L_O$ and starting material feed rate Fi (L_O represents filler length before kneading). For the stainless steel fiber filler, high values of $\bar{L}_F/L_O$ were obtained at high feed rates. Under these conditions, $\bar{\rho}_v$ had low values, as seen in Figure 6. This demonstrates that an increase in filler length results in an increased probability of filament-to-filament contact and hence excellent electroconductivity. In the case of the glass fiber filler, however, the filler length was much shorter than that of the stainless steel fiber filler, and the change in the filler length is negligible in comparison with Fi.

This is attributable to the fact that glass fiber filler is prone to damage upon kneading, as stated above; apparently, filler length has no effect on electroconductivity. However, examination of filler length on an increased scale as shown in Figure 8 showed that filler length increased as Fi increased in the case of the glass fiber filler as well. It was thus confirmed that electroconductivity increases as filler length increases also for the glass fiber filler.

Figure 9 shows the relationship between dimensionless mean filler length $\bar{L}_F/L_O$ and
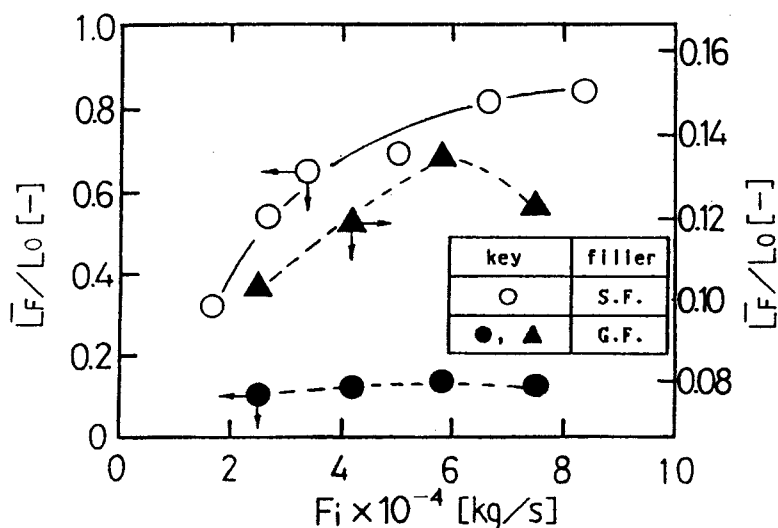

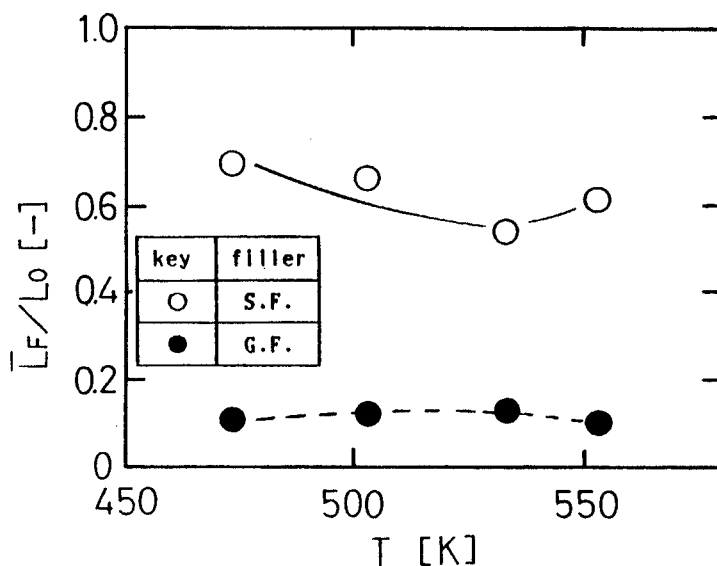Fig. 8 The relationship between dimensionless mean filler length $\bar{L}_F/L_O$ and starting material feed rate Fi.

Fig. 9 The relationship between dimensionless mean filler length $\bar{L}_F/L_O$ and kneading temperature T.

Keijiro TERASHITA, Tetsuya TANAKA, Kiyohiko NISHIMURA
and Kei MIYANAMI

kneading temperature T. For both the stainless steel fiber filler and glass fiber fill-er, $\bar{L}_F/L_O$ decreased or remained almost unchanged with the rise in T. However, this finding, combined with the fact that electroconductivity increased as kneading temper-ature increased as seen in Figure 7, suggests that electroconductivity depends largely on the effect of dispersion rather than on filler length.

b) Effect of filler distribution state on electroconductivity

As stated above, the keys to design of an excellently electrically conductive compo-site material are a uniform filler distribution (bundled filler filaments are separated and distributed throughout the matrix resin) and unbiased filler orientation (filler filaments are oriented in every direction). Thus the filler dispersion state mentioned herein generically involves the distribution state and orientation state. Quantitative representation of these two states is important in designing an excellently electrically conductive composite material.

The fractal dimension was used as an index of filler distributuion state (the degree of filler filament separation). As stated in term 2.2.c), use of fractal dimension D allows a quantitative representation of visible filler distribution state, i.e., the distri-bution state improves as D increases.

Figure 10 shows the relationship between fractal dimension D and starting material feed rate Fi. D remained almost unchanged independent of Fi($Fi \leqq 6.67 \times 10^{-4}$ kg/s for the stainless steel fiber filler, $Fi \leqq 5.83 \times 10^{-4}$ kg/s for the glass fiber filler). This demonstrates that the filler distribution state (the degree of separation) is not affect-ed by Fi after the filler filaments have been separated to some extent. However, when Fi had a high value ($Fi = 8.33 \times 10^{-4}$ kg/s for the stainless steel fiber filler, $Fi = 7.50 \times 10^{-4}$ kg/s for the glass fiber filler), kneaded products were found to contain ag-
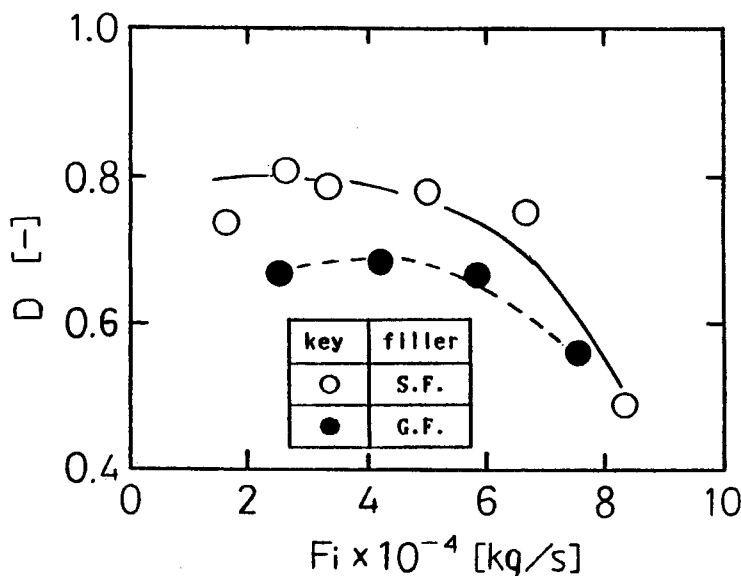

Fig. 10 The relationship between fractal dimension D and starting material feed
rate Fi.

gregated filler filament bundles due to insufficient resin melting, with low values for D(D=0.4919 for the stainless steel fiber filler, D=0.5597 for the glass fiber filler).

Figure 11 shows the relationship between fractal dimension D and kneading temperature T. For both types of fillers, D increased as T increased. It can therefore be thought that the filler distribution betters as kneading temperature increases. Combined with the showing of Figure 7 (electroconductivity improved as D increased), this finding suggests that under these conditions (T changes), electroconductivity is significantly affected by the filler distribution state.
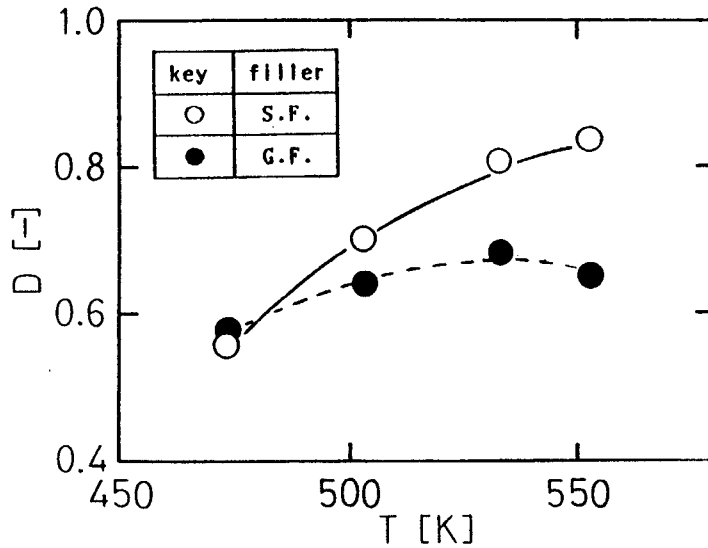

Fig. 11 The ralationship between fractal dimension D and kneading temperature T.

c) Effect of filler orientation state on electroconductivity

As an index of filler orientation state or the degree of randomization of fibrous filler orientation, the direction ratio was used. This parameter is defined as the ratio of volume specific resistivities obtained in two directions as described in term 2.2.a), indicating filler orientation. Direction ratio R can be written as follows:

$$R = (\Sigma(\rho_{1i}/\rho_{2i}))/15 \qquad \cdots\cdots (3\text{-}1)$$

where $\rho_{1i} > \rho_{2i}$, R being the mean for 15 samples. It can be speculated that as R approximates to 1, the filler orientation state improves with filler dispersion in every direction.

Figure 12 and 13 show the relationships between direction ratio R and feed rate Fi and between R and kneading temperature T, respectively. From these figures, it is seen that R decreased as Fi increased or T increased for the stainless steel fiber filler. For the glass fiber filler, R remained almost unchanged independent of operating conditions. The filler filling ratio, based on percent volume ratio, was 1.44 vol% for the

Keijiro TERASHITA, Tetsuya TANAKA, Kiyohiko NISHIMURA
and Kei MIYANAMI

stainless steel fiber filler and 16.15 vol% for the glass fiber filler, over 10 times high-
er than for the stainless steel fiber filler. In other words, since the glass fiber filler
was present very dense in the matrix resin, the probability of filler filament contact
was higher than in the stainless steel fiber filler, accounting for the lower R values in
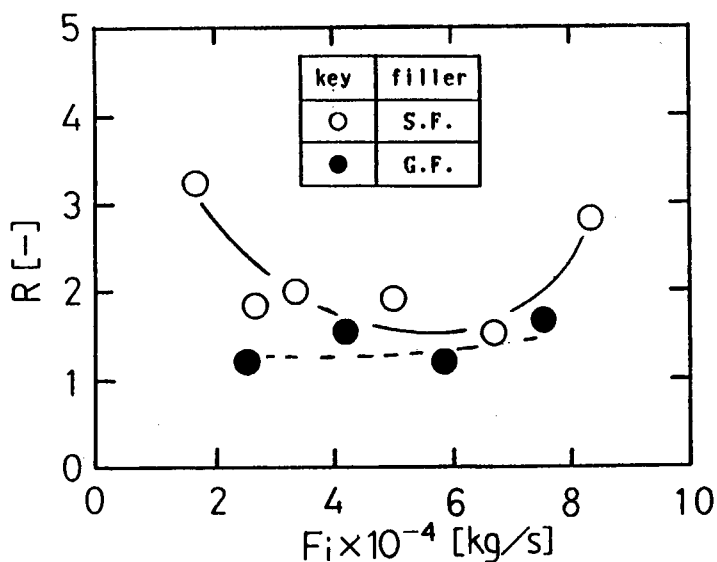the glass fiber filler.

Fig. 12 The relationship between direction ratio R and starting material feed
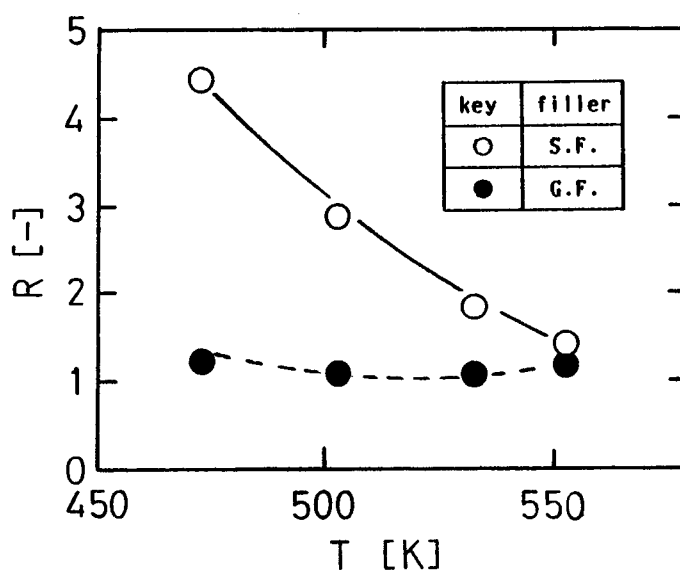rate Fi.

Fig. 13 The relationship between direction ratio R and kneading temperature T.

These findings demonstrate that long filler length is retained at high starting material feed rates. Also, the filler distribution state improved as kneading temperature increased, with little influence of feed rate. Moreover, the filler orientation state improved as the feed rate increased or kneading temperature increased.

Next examind were the relationships between electroconductivity and a number of factors involved in the formation of electrically conductive network, namely filler length, fractal dimension and direction ratio. Figure 14 shows the effect of the product $D \cdot (\bar{L}_F/L_O)/R$ of dimensionless mean filler length $\bar{L}_F/L_O$, fractal dimension D and the reciprocal of direction ratio R on Volume specific resistivity $\bar{\rho}_v$. The $D \cdot (\bar{L}_F/L_O)/R$ serves as an index of the formation of electrically conductive network; a higher value results in a better electrically conductive network. From Figure 14, it is seen that $\bar{\rho}_v$ decreased as the $D \cdot (\bar{L}_F/L_O)/R$ increased. It was thus possible to assess the relationship between the electroconductivity of an electrically conductive composite resin and network formation, irrespective of the filler used, on the basis of the product $D \cdot (\bar{L}_F/L_O)/R$ of network formation factors $\bar{L}_F/L_O$, D and $1/R$.
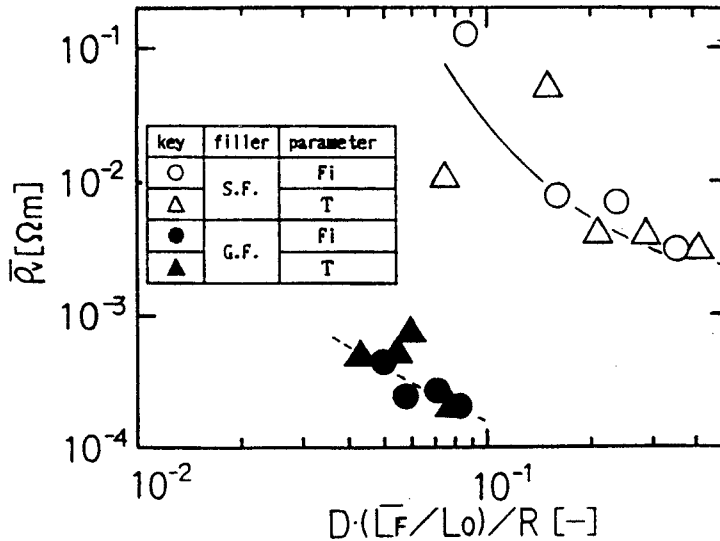

Fig. 14   The effect of product $D \cdot (\bar{L}_F/L_O)/R$ of dimensionless mean filler length L_F/L_O, fractal dimension D and the reciprocal of direction ratio R on volume specific resistivity $\bar{\rho}_v$.

3. 3.   Relationship between network formation factors and fluididty

This section discusses the relationship between factors involved in the formation of electrically conductive network and kneaded product fluidity.

Figure 15 shows the relationship between dimensionless mean filler length $\bar{L}_F/L_O$ and the total number Nt of paddle revolutions during the mean residence time of kneaded materials. Nt was obtained as follows:

$$Nt = N \times \bar{t} \qquad \cdots \cdots (3\text{-}2)$$

Keijiro TERASHITA, Tetsuya TANAKA, Kiyohiko NISHIMURA
                          and Kei MIYANAMI

where N is the paddle revolution rate, and $\bar{t}$ is the mean residence time of kneaded materials in the kneading vessel. From Figure 15, it is seen that $\bar{L}_F/L_O$ decreased as Nt increased (70 to 180) for the stainless steel fiber filler. For the glass fiber filler, $\bar{L}_F/L_O$ remained almost unchanged at 0.1 to 0.3, since the total number of revolutions was almost constant (Nt=20 to 25). The filler is thought to be cut by the mechanical shearing action of the kneading paddles and the compressing/elongating action of convecting resin. Since stainless steel fiber filler length was affected directly by the total number of revolutions, as seen from the figure, it is speculated that the shearing action of the kneading paddles is dominant in filler cutting. In the case of the glass fiber filler, $\bar{L}_F/L_O$ appears to be decreased by the shearing action of the kneading paddles and the compressing/elongating action of convecting resin, despite the low value of Nt, since the glass fiber filler is prone to damage.
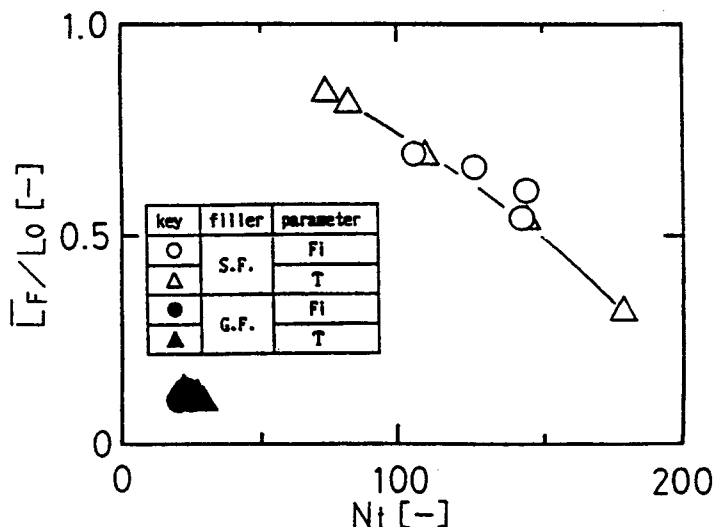

Fig. 15 The relationship between dimensionless mean filler length $\bar{L}_F/L_O$ and the total number Nt of paddle revlutions during the mean residence time of kneaded materials.

As for the factors affecting the filler distribution state (the degree of filler filament separation), the filler distribution state improved as kneading temperature increased, as is evident from Figure 11. The filler distribution state remained almost unchanged when kneading temperature was constant. This is probably because the fluidity of the feed in the kneading vessel significantly affected the filler dispersion at the kneading temperature. Among the factors involved in molten resin fluidity are apparent resin melt viscosity μ and kneading paddle shearing stress τ. The relationship between resin fluidity and filler distribution was examined. Figure 16 shows the relationship between fractal dimension D and the ratio τ/μ of shearing stress τ to resin viscosity μ. τ is expressed as follows:

$$\tau = Tq/Vh \qquad\qquad \cdots\cdots (3\text{-}3)$$

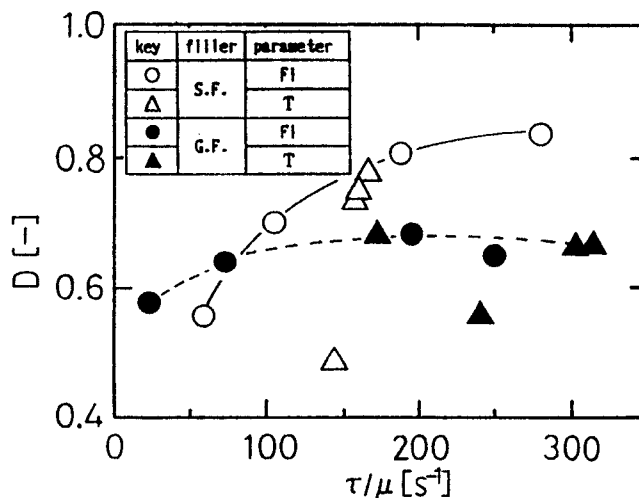| key	filler	parameter
○	S.F.	Fl
△		T
●	G.F.	Fl
▲		T

Fig. 16   The relationship between fractal dimansion D and the ratio τ / μ of
shearing stress τ to resin viscosity μ.

where Tq represents kneading torque and Vh represents the kneaded material holdup in
the kneading vessel.   From Figure 16, it is seen that fractal dimension D increases as
τ / μ increases.   In other words, the filler distribution state improves as shearing
stress increases and apparent melt viscosity decreases.

Finally, the factors affecting filler orientation are discussed.   The orientation state
is the direction of fibrous filler, as stated above.   It is therefore necessary to facili-
tate macroscopic migration of filler in the resin to ensure random orientation of the
filler.   For such macroscopic migration and mixing, it is important to facilitate the
fluidization of the kneaded materials by reducing the apparent melt viscosity of the
resin and to increase the holdup to exert sufficient shearing action on the kneaded ma-
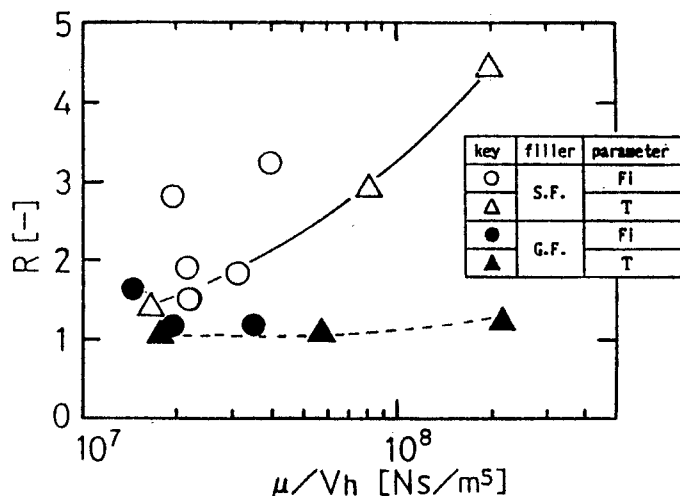terials.   Figure 17 shows the relationship between direction ratio R and μ /Vh.   When

key	filler	parameter
○	S.F.	Fl
△		T
●	G.F.	Fl
▲		T

Fig. 17   The relationship between direction ratio R and μ /Vh.

the glass fiber filler was used, R remained almost unchanged, due to the high filler filling ratio, as stated above. In the case of the stainless steel fiber filler, R decreased as μ /Vh decreased. In short, good orientation is obtained when the apparent resin viscosity is low and the holdup is high.

4. Conclusion

In an attempt to quantitavely assess the dispersion state of filler in matrix resin, two kinds of fibrous electrically conductive fillers were continuously kneaded to yield an electrically conductive composite resin. The filler dispersion state and filler orientation state, distribution forming factors, could be quantitatively assessed by fractal dimension D and direction ratio R, respectively. The electroconductivity of an electrically conductive composite resin was proved to depend on the relationship among filler length $\bar{L}_F/L_O$, filler dispersion state and filler orientation state, rather than on filler type, i.e., an excellently electrically conductive composite resin is obtained when $D \cdot (L_F/L_O)/R$ has a high value.

Operating factors for design of an excellently electrically conductive composite material were examined. A good filler distribution and orientation, with long filler length, are obtained when the number of paddle rotations Nt is low, the ratio τ / μ of shearing stress τ to resin viscosity μ is high, and the ratio μ /Vh of μ to holdup Vh is low.

Nomenclature

A	= total area of the segment	[m²]
Af	= area of the filler region in a single segment	[m²]
D	= fractal dimension	[−]
Ds(n)	= coefficient of variance	[−]
Fi	= atarting material feed rate	[kg/s]
Iw	= filling ratio	[wt%]
L_O	= filler length before kneading	[m]
L_F	= filler length	[m]
l	= distance between electrode	[m]
N	= paddle revolution rate	[s⁻¹]
Nt	= total number of paddle revolutions during the mean residence time of kneaded materials	[−]
n	= number of division	[−]
R	= direction ratio	[−]
R_v	= residence value	[Ω]
S	= cut area	[m²]

Sf	= area ratio of filler	[—]
$\overline{Sf}$	= mean area ratio of filler	[—]
T	= kneading temperature	[K]
Tq	= kneading torque	[J]
$\bar{t}$	= mean residence time of kneaded materials in kneading vessel	[s]
Vh	= keaded material holdup in the kneading vessel	[m³]
$\sigma s(n)$	= standard deviation of Sf	[—]
ρ_v	= volume specific resistivity	[Ω・m]
$\overline{\rho_v}$	= mean volume specific resistivity	[Ω・m]
τ	= kneading paddle shearing stress	[N/m²]
μ	= apparentresin melt viscosity	[Pa・s]

References

1) K. Terashita, M. Mitsui, P. J. Lyoo and K. Miyanami: Zairyo, **38**, 1452 (1989)

2) P. J. Lyoo, K. Terashita, M. Mitsui and K. Miyanami: Funtaikogakukaishi, **26**, 684 (1989)

3) P. J. Lyoo, K. Terashita and K. Miyanami: Funtaikogakukaishi, **27**, 140 (1990)

4) K. Terashita, Y. Mizuno, P. J. Lyoo and K. Miyanami: Kagakukogaku Ronbunsyu, **16**, 715 (1990)

5) Y. Mizuno, K. Terashita, Y. Kondo and K. Miyanami: Kagakukogaku Ronbunsyu, **18**, 58, (1992)

6) Y. Mizuno, K. Terashita and K. Miyanami: Kagakukogaku Ronbunsyu, **18**, 58, (1992)

7) T. Aratani, T. Fujii, T. Morikawa and K. Miyanami: Kagakukogaku Ronbunsyu, **14**, 395 (1992)

8) M. Suzuki, Y. Muguruma, M. Hirota and T. Oshima: Funtaikogakukaisyi, **25**, 287 (1988)

9) M. Suzuki and T. Oshima: Funtaikogakukaishi, **26**, 4 (1989)